Design and analysis of a brushless DC motor for applications in robotics

Article *in* IET Electric Power Applications · December 2012

DOI: 10.1049/iet-epa.2011.0267

CITATIONS
35

READS
3,433

4 authors, including:

Ping Lun Li
Industrial Technology Research Institute
14 PUBLICATIONS **287** CITATIONS
SEE PROFILE

Cheng-Tsung Liu
National Sun Yat-sen University
146 PUBLICATIONS **1,013** CITATIONS
SEE PROFILE

Published in IET Electric Power Applications
Received on 23rd August 2011
Revised on 15th April 2012
doi: 10.1049/iet-epa.2011.0267

ISSN 1751-8660

Design and analysis of a brushless DC motor for applications in robotics

C.C. Hwang[1] *P.L. Li*[2] *C.T. Liu*[3] *C. Chen*[4]

[1]*Department of Electrical Engineering, Feng Chia University, Taichung 407, Taiwan*
[2]*Ph.D. Program in Electrical and Communications Engineering, Feng Chia University, Taichung 407, Taiwan*
[3]*Department of Electrical Engineering, National Sun Yat-sen University, Kaohsiung 804, Taiwan*
[4]*Pan-World Control Tech., Inc., Taipei 104, Taiwan*
E-mail: cchwang@fcu.edu.tw

Abstract: This study presents the design of a three-phase slotless brushless DC (BLDC) motor for use as an electromagnetic actuator in robotics. To achieve the high torque-to-inertia and torque-to-weight ratios required for fast response in robotic applications, genetic algorithms (GAs) are used to optimise the initial motor design within a reasonable geometry. We examine the machine performance using 3-D finite element analysis (FEA) and validate them by experimental measurement.

1 Introduction

Brushless DC (BLDC) motors have attracted significant interest for applications in robotics because of their large torque-producing capability, high reliability and low maintenance [1–5]. To satisfy the miniaturisation requirement for applications in robotics, a motor with a slotless stator and a rotor equipped with high-energy permanent magnets (PMs), such as neodymium iron boron (NdFeB) or samarium–cobalt (SmCo) magnets, is one of the most common configurations for use as an electromagnetic actuator in current robotics.

Two common winding arrangements employed in miniature slotless BLDC motors are axial and non-axial windings. Faulhaber, rhombic and zigzag windings are examples of non-axial windings [6–8]. One important advantage of these windings is a short-end connection. However, they have been patented [9, 10] and the tooling and manufacturing processes needed for their construction are not any easier. In this study, single-layer short-pitch windings were employed. Since the stator consists of a simple cylinder without any slots, the pre-wound axial windings could easily be attached and fixed to the inner surface of the cylinder using glue or epoxy. This enables easier manufacturing of this kind of miniaturised machines [11, 12].

The two-pole rotor and three-phase slotless stator discussed above, with a single-layer short-pitch windings motor was, designed based on the well-established computerised design procedures [3–5, 13]. Moreover, to achieve the high torque-to-inertia and torque-to-weight ratios required for fast response in robotic applications, genetic algorithms (GAs) were utilised for the design optimisation of the motor within a reasonable geometry [14–16]. Finally, a prototype motor was fabricated and tested to confirm the computational results which were revealed to be in good agreement.

2 Model of the motor

The initial design of a three-phase, 12 V, 5 W, 6000 rpm, two-pole PM motor is shown in Fig. 1. The motor consists of a slotless stator that accommodates the single-layer short-pitch windings, and a sintered two-pole NdFeB magnet rotor with parallel magnetisation. The stator laminations are made of non-oriented silicon steel with a saturated flux density (B_s) of 1.7 T. The rotor consists of a unique cylindrical magnet with a remanence (B_r) of 1.445 T and a relative recoil permeability (μ_r) of 1.05, and a ferromagnetic shaft. The initial design of the machine parameters is given in Table 1. Since the rotor length-to-diameter is less than 3, no retaining sleeve is required around the magnets for the desired application [11]. The conductors are spread in the winding segment as shown in Fig. 1. Each phase covers 120 electrical degrees with the bobbin angle β between the positive (e.g. $A+$) and negative (e.g. $A-$) winding segments. The angle is introduced for the phase winding wounding on a bobbin before it is inserted into the stator. The angle size does not affect the performance of the motor because the amount of flux linkage that can be generated in the region is very small, especially for a low number of poles [12, 17]. In this study, the angle β was fixed at 5 electrical degrees.

3 Genetic algorithms

Any optimisation procedure involves finding a vector $\boldsymbol{X} = (x_1, x_2, \ldots, x_n)$, representing a set of n design variables, each of them bounded by $x_{im} \leqq x_i \leqq x_{in}$, i, $i = 1, 2, \ldots, n$, so that the objective function $F(\boldsymbol{X})$ is

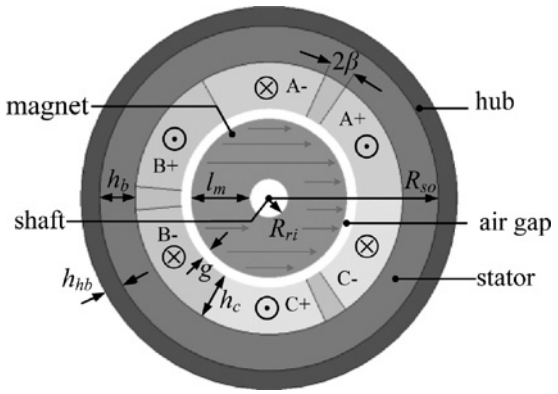

Fig. 1 *Initial design of the motor*

Table 1 Machine parameters

Parameter	Symbol	Value
copper wire mass density	ρ_{sw}	8900 kg/m^3
core mass density	ρ_{sc}	7650 kg/m^3
magnet mass density	ρ_{pm}	7400 kg/m^3
shaft mass density	ρ_{sh}	7800 kg/m^3
hub mass density	ρ_{hb}	7930 kg/m^3
hub outer radius	R_{hb}	11 mm
rotor outer radius	R_{ro}	4.5 mm
rotor inner radius	R_{ri}	1.5 mm
stator outer radius	R_{so}	10 mm
stator stack length	L_s	21 mm
shaft length	L_{sh}	30 mm
rotor length	L_r	20 mm
hub axial length	L_{hb}	25 mm
hub thickness	h_{hb}	1 mm
radial winding thickness	h_c	2.8 mm
stator back iron width	h_b	2.2 mm
mechanical air gap length	G	0.5 mm
number of turns per phase	N_t	94

maximised (or minimised), while satisfying a set of k constraints $G_j(\boldsymbol{X}) \leqq 0$, $j = 1, 2, \ldots, k$ [14–16]. In this paper, GA optimisation was applied to the design of a slotless BLDC motor to maximise the torque-to-inertia and torque-to-weight ratios.

3.1 Objective function

The rotor inertia and motor weight are taken as the objective functions to be minimised for a rated torque not less than the specified value. The rotor inertia (J) is defined as

$$J = F_1(x_i) = \frac{\pi}{2}[L_s\rho_{pm}(R_{ri} + l_m)^4 + L_{sh}\rho_{sh}R_{ri}^4] \quad (1)$$

where ρ_{pm} and ρ_{sh} are the specific mass densities of magnet and shaft, respectively, L_s and L_{sh} are the axial stack lengths of stator and shaft, respectively, R_{ri} is the radius of shaft and l_m is the magnet thickness. The motor weight (M) is the sum of the stator, rotor, magnet and winding weights and is given by

$$\begin{aligned} M = F_2(x_i) = {} & [R_{so}^2 - (R_{so} - h_b)^2]\rho_{sc}\pi L_s + R_{ri}^2\rho_{sh}\pi L_{sh} \\ & + \left[2L_s + \frac{\pi^2(R_{ri} + l_m + g + h_c/2)}{3}\right]N_{ph}N_tA_w\rho_{sw} \\ & + [(l_m + R_{ri})^2 - R_{ri}^2]\rho_{pm}\pi L_r \\ & + [(R_{so} + h_{hb})^2 - (R_{so})^2]\rho_{hb}\pi L_s \\ & + 2[(R_{so} + h_{hb})^2 - R_{ri}^2]\rho_{hb}\pi h_{hb} \end{aligned} \quad (2)$$

where ρ_{sc} and ρ_{sw} are the specific mass densities of the stator core and copper, respectively, h_c is the winding segment thickness, A_w is the cross-sectional area of a conductor, N_{sh} is the number of parallel paths, N_t is the number of turns in series per phase and N_{ph} is the number of phases.

3.2 Variables and their limits

In this study, six geometrical variables were defined as design variables, $x_1 = l_m$, $x_2 = h_b$, $x_3 = h_c$, $x_4 = R_{ri}$, $x_5 = g$ and $x_6 = k_f$. Here, k_f is the winding filling factor. The remaining design parameters can be expressed in terms of the above variables or assigned fixed values.

According to the geometry of the motor and the materials used, the bounds of the design variables can be expressed as

$$\begin{aligned} & 2 \leq x_1 \leq 3.5;\ 1.8 \leq x_2 \leq 2.5;\ 2.5 \leq x_3 \leq 3.5 \\ & 1 \leq x_4 \leq 2;\ 0.5 \leq x_5 \leq 0.8;\ 0.5 \leq x_5 \leq 0.8;\ 0.5 \\ & \leq x_6 \leq 0.9 \end{aligned} \quad (4)$$

Maintaining the flux density through the stator back iron below the core saturation of 1.7 T, gives

$$\frac{\pi k_l \alpha B_r l_m}{2h_b \ln((R_{ri} + l_m + g + h_c)/(R_{ri}))} \leq 1.7 \quad (5)$$

where α is the pole arc to pole pitch ratio and k_l is a leakage factor which can be approximated by [18]

$$k_l = 1 - \frac{1}{1 + 0.9[(R_{ri} + l_m)/(\alpha(g + h_c))]^2} \quad (6)$$

Considering the demagnetisation curve of the NdFeB magnet as a straight line in the second quadrant with relative recoil permeability μ_r, B_g can be calculated as [18]

$$B_g = \frac{k_l B_r l_m}{(R_{ri} + l_m + g)\ln((R_{ri} + l_m + g + h_c)/(R_{ri}))} \quad (7)$$

The number of turns per phase N_t can be expressed as

$$N_t = \frac{A_{sp}}{N_{sh}A_w}k_f \quad (8)$$

where A_{sp} is the cross-sectional area occupied by one winding segment.

If the converter is supplied by an ideal direct voltage source V, then at any instant the following equation should be satisfied

$$V \geq E_{L-L} + 2I_{ph}R_{ph} \quad (9)$$

where I_{ph} is the phase current and the line-to-line back-EMF (E_{L-L}) is given by [13]

$$E_{L-L} = \sqrt{3}\,k_w N_{sp} B_g N_t (R_{ri} + l_m + g + h_c) L_s \omega_m \quad (10)$$

doi: 10.1049/iet-epa.2011.0267

where ω_m is the rotor speed, and the resistance per phase (R_{ph}) is given by

$$R_{ph} = \rho_R N_{WS}\left[2L_s + \frac{\pi}{3}\left(R_{ri} + l_m + g + \frac{h_c}{2}\right)\right]/(N_{sh}N_t A_w) \quad (11)$$

where ρ_R is the resistivity of conductor and N_{WS} is the number of winding segment pairs per phase.

Another constraint is that the motor torque (T) is not less than 8 mN m and is given as follows

$$T = \frac{3}{\sqrt{2}}\frac{\pi(l_m + R_{ri} + g)L_s B_g k_w N_t I_{ph}}{2} \geq 0.008 \quad (12)$$

where k_w is the winding factor.

The last constraint is that the outer radius of stator (R_{so}) is not greater than 10 mm,

$$10 \geq R_{so} = R_{ri} + l_m + h_b + h_c + g \quad (13)$$

4 Result and discussions

In this study, a program based on GAs was constructed and results were obtained after 36 iterations when setting the population size to be 200 for each parameter, and the crossover and mutation rates to be 0.95 and 0.1, respectively. The machine performance characteristics were obtained from 3-D finite element analysis (FEA) using Magsoft software [19]. Fig. 2 shows the photographs of the prototype motor. Fig. 3 shows the magnetic flux distribution within the motor under the no load condition. It shows that there is no flux above the level of saturation within the motor. Fig. 4 shows the simulated result of the air gap flux density under no load. As anticipated, with parallel magnetisation, the flux density distribution in the air gap is nearly sinusoidal. The back-EMF is an important parameter in robotics because of the power limitations. The analytical solution of line-to-line back-EMF was found to be 4.214 V (RMS) at 6000 rpm by employing (10). The simulated and measured waveforms of back-EMFs at 6000 rpm have similar sinusoidal waveforms as shown in Fig. 5. They are in agreement with each other. Moreover, the measured waveform of back-EMF has a peak of 6.08 V that meets the specifications.

The design parameters and the performances of the initial design and the GA-optimised design are compared in Table 2. It shows that the torque-to-inertia ratio and the torque-to-weight ratio increase from 8.6339×10^4 N/kg m and 0.2132 N m/kg in the initial design to

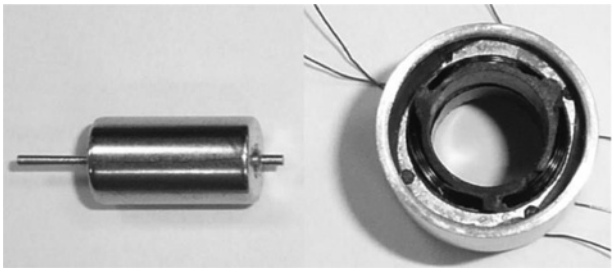

Fig. 2 *Photographs of the realised prototype*

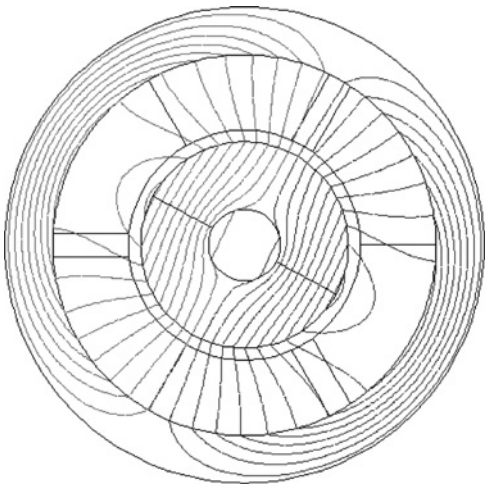

Fig. 3 *Magnetic flux distribution*

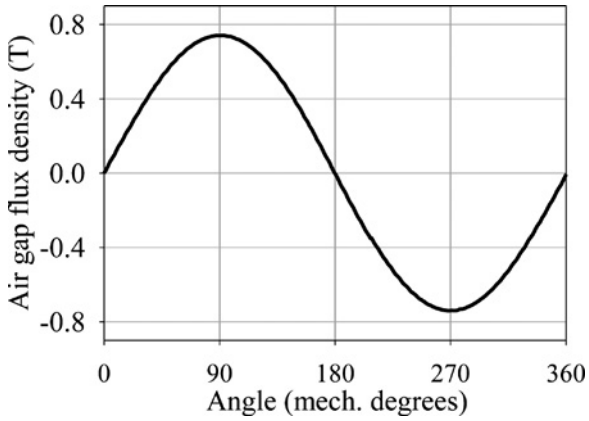

Fig. 4 *Air gap flux density under no load*

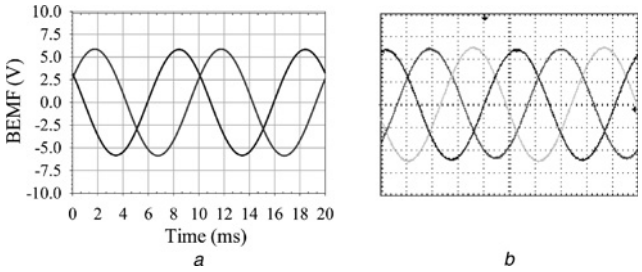

Fig. 5 *Line-to-line back-EMF waveforms at 6000 rpm*

a Simulated back-EMF
b Measured back-EMF
Both traces have 2.5 V/division and 2 ms/division

Table 2 Comparison of design parameters

Parameter	Initial	GAs
l_m, mm	3	3.2508
h_b, mm	2.2	1.9567
h_c, mm	2.8	2.5022
R_{ri}, mm	1.5	1.0006
g, mm	0.5	0.5
k_f	0.5639	0.6864
N_t, turns	94	96
T, N m	8.345×10^{-3}	8.684×10^{-3}
J, kg m^2	9.6654×10^{-8}	7.6192×10^{-8}

Table 3 Comparison of volume, weight and costs

Item	Initial		GAs		Price, USD/kg
	Volume, cm^3	Weight, g	Volume, cm^3	Weight, g	
magnet	1.131	8.3694	1.072	7.9382	531.3661
copper	1.2179	10.8389	1.2159	10.8211	13.2203
iron	2.5898	19.7639	2.0241	16.2588	1.7288
shaft	0.2121	1.6541	0.0629	0.736	5.0847
hub	2.8932	22.1501	2.4779	19.6521	4.2373
total	8.044	62.7764	6.8528	55.4062	—
cost	4.7269 USD	—	4.4763 USD	—	—

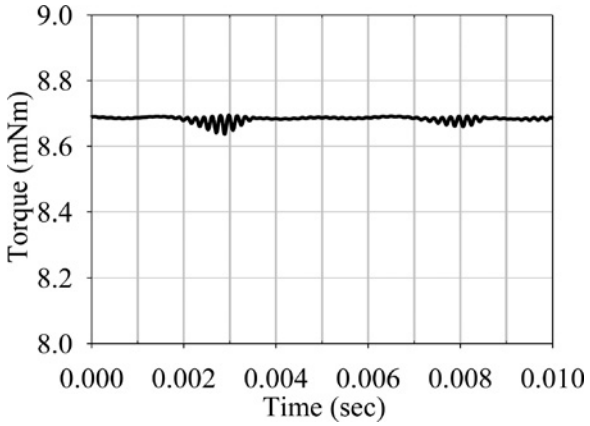

Fig. 6 *Torque waveform*

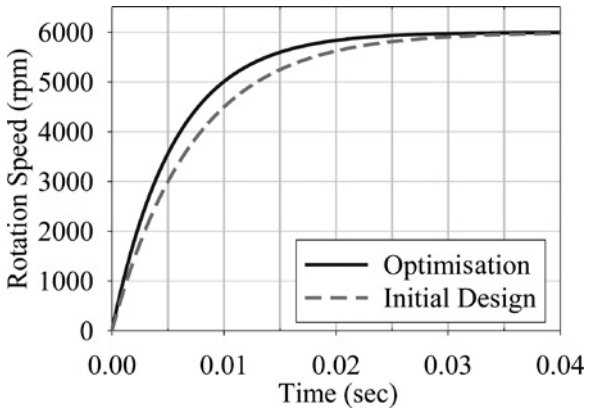

Fig. 7 *Speed against time response*

11.3975×10^4 N/kg m and 0.25 N m/kg in the GAs, respectively. These results confirm that the optimisation is of benefit to the motor to speed up masses of robotics. In addition, we can also compare the active materials' volume, weight and cost between the initial design and the GAs from the simulation as shown in Table 3. As the table shows, the volume, weight and cost reduce from the initial design of 8.044 cm^3, 62.7764 g and 4.7269 USD to the GAs of 6.8528 cm^3, 55.4062 g and 4.4763 USD. The volume and weight are reduced by 14.8 and 11.74%, respectively. Again, this illustrates that the motor size and manufacturing costs through the GAs are reduced by the use of the GAs.

It is worth investigating the variation of current with torque to compute the torque constant that couples the electrical circuit equations with the mechanical equations. The torque constant was found to be 10.098 mN m/A. We can also address the instantaneous torque from the simulation. Fig. 6 shows the torque waveform. The average torque is found to be 8.684 mN m with a 0.63% torque ripple, which meets

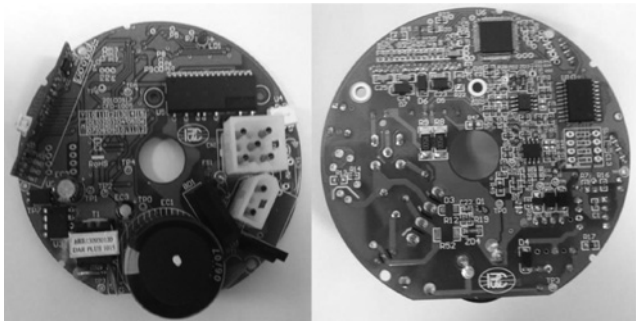

Fig. 8 *Prototyped controller using Infineon XC886CM*

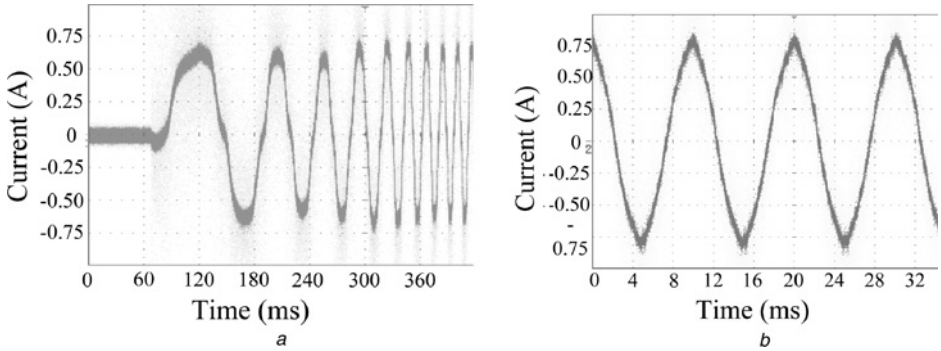

Fig. 9 *Phase current (6000 rpm)*

a At motor starting stage
b At steady running stage

doi: 10.1049/iet-epa.2011.0267

the specifications. The speed against time for the motor startup is shown in Fig. 7. From this figure, the mechanical time constant is found to decrease from 7.1823 ms in the initial design to 5.521 ms in the GAs. This value can result in a suitable motor startup performance.

5 Experimental tests

Owing to the rapid progress of semiconductor manufacturability, the state-of-art field oriented control (FOC) algorithm can be implemented using a low-cost 8-bit MCU such as the Infineon XC886/888 series. The FOC-based controller also exhibits higher efficiency, better dynamic response and fewer torque harmonics and it perfectly matches with the motor design having the sinusoidal back-EMF. In this paper, the prototype controller (see Fig. 8) has been tested with the designed motor.

The phase current waveforms for motor startup and for steady running at 6000 rpm were observed. Fig. 9*a* shows the successful startup of the motor after a few cycles. Fig. 9*b* shows the near sinusoidal waveform of phase current. The slight distortion of this current waveform is acceptable on account of it having less motor noise and vibration compared with the square waveform.

6 Conclusions

The design of a three-phase slotless BLDC motor drive for use as an electromagnetic actuator in robotics is presented. The GAs are utilised for the design optimisation to achieve the high torque-to-inertia and torque-to-weight ratios required for fast response in robotic applications. The prototype motor drive has been constructed and tested, validating the theoretical design and analysis.

7 References

1 Bassi, E., Benzi, F., Dallago, E., Fabrizi, D., Fabrizi, G.: 'A mechanical simulator for testing and evaluating electrical drives for robotics applications'. Conf. Record of IEEE IAS Annual Meeting, Dearborn, USA, September–October 1991, vol. 2, pp. 1414–1420

2 Williams, S.: 'Direct drive system for an industrial robot using a brushless DC motor', *IEE Proc. B*, 1985, **132**, (1), pp. 53–56

3 Hesmondhalgh, D.E., Tipping, D.: 'Slotless construction for small synchronous motors using samarium cobalt magnets', *Proc. IEE-Elect. Power Appl.*, 1982, **129**, (5), pp. 251–261

4 Bianchi, N., Bolognani, S., Luise, F.: 'Potentials and limits of high speed PM motors', *IEEE Trans. Ind. Appl.*, 2004, **IA-40**, (6), pp. 1570–1578

5 Chabban, F.B.: 'Determination of the optimum rotor/stator diameter ratio of permanent magnet machines', *Elect. Mach. Power Syst.*, 1994, **22**, pp. 521–531

6 Hur, J., Rhyu, S.H., Jung, I.S., Sung, H.G., Kown, B.I.: 'Three-dimensional characteristic analysis of micro BLDC motor according to slotless winding shape', *IEEE Trans. Magn.*, 2003, **39**, (5), pp. 2989–2991

7 Ragot, P., Marosvic, M., Perriard, Y.: 'Analytical determination of the phase inductances of a brushless DC motor with faulhaber winding', *IEEE Trans. Ind. Appl.*, 2010, **46**, (4), pp. 1360–1366

8 Dehez, B., Marosvic, M., Perriard, Y.: 'Analysis of BLDC motor with zigzag and rhombic winding'. Int. Conf. ICEM Rome, Italy, 2010, pp. 1–5

9 Faulhaber, F.: 'Armature winding for rotary electrical machines'. US Patent 3360668, December 1967

10 Rohrer, R., Schulze, J., Hofer, R.: 'Electric motor with multilayered rhombic single coils made of wire'. US Patent 0103025, October 2006

11 Bianchi, N., Bolognani, S., Luise, F.: 'High speed drive using a slotless PM motor', *IEEE Trans. Power Electron.*, 2006, **21**, (4), pp. 1083–1090

12 Marosvic, M., Perriard, Y.: 'Simplified design methodology for a slotless brushless DC motor', *IEEE Trans. Magn.*, 2006, **42**, (12), pp. 3842–3846

13 Miller, T.J.E.: 'Brushless permanent magnet and reluctance motor drives' (Clarendom Press, 1989, 1st edn.)

14 Hwang, C.C., Lye, L.Y., Liu, C.-T., Li, P.L.: 'Optimal design of an SPM motor using genetic algorithms coupled Taguchi method', *IEEE Trans. Magn.*, 2008, **44**, (11), pp. 4325–4328

15 Bianchi, N., Bolognani, S.: 'Design optimization of electric motors by genetic algorithms', *IEE Proc. B, Electr. Power Appl.*, 1998, **145**, (5), pp. 475–483

16 Chung, T.K., Kim, S.K., Hahn, S.Y.: 'Optimal pole shape design for the reduction of cogging torque of brushless DC motor using evolution strategy', *IEEE Trans. Magn.*, 1991, **33**, (2), pp. 1908–1911

17 Wallamrk, O., Kjellqvist, P.: 'Analysis of a low-cost air-gap winding for permanent magnet synchronous motors', *IEEE Trans. Energy Convers.*, 2009, **24**, (4), pp. 841–847

18 Rahideh, A., Korakiantis, T., Ruiz, P., Keeble, T., Rothman, M.T.: 'Optimal brushless DC motor design using genetic algorithms', *J. Magn. Magn. Mater.*, 2010, **322**, (22), pp. 3680–3687

19 'Flux user's guide, version 10.4.2' (Magsoft Corporation, Ballston Spa, New York, 2011)